FATIGUE BEHAVIOUR PREDICTION OF LASER SURFACE TREATED ALUMINIUM PLATES THROUGH SIMULATION OF THE LASER STRIPPING PROCESS

G. Labeas[1], S. Tsirkas[2], Al. Kermanidis[1] and Sp. Pantelakis[1]

[1]LTSM, Laboratory of Technology and Strength of Materials
Department of Mechanical Engineering & Aeronautics
University of Patras, Patras 26500, GREECE
[2]ISTRAM, Institute of Structures and Advanced Materials
Patron-Athinon 57, Patras 26441, GREECE

ABSTRACT

Laser techniques are currently applied in a series of engineering processes due to their technological and economic advantages. Characteristic applications are the cutting of complex shapes, drilling on curved surfaces, welding of dissimilar metals, surface treatment etc. In the present work the numerical simulation of the laser paint removal process, which aims on the understanding of the fatigue behaviour of laser surface treated plates, is presented. The application of laser radiation (carbon dioxide and excimer) is associated with significant fatigue life extension. The observed enhancement of fatigue life is attributed to the development of compressive residual stresses during the paint removal processing. To enable prediction of the fatigue behaviour of the surface treated material, a numerical model is developed for simulation of the laser paint removal process. The model is based on a nonlinear transient coupled thermal-structural analysis and accounts for the temperature dependency of the thermal and mechanical properties of the material. The model is applied in the calculation of the residual stresses of the paint removal process. The simulation results correlate well with the experimental results and enable prediction of the fatigue behaviour of the laser treated material, based on the fatigue curves of the original material.

1. INTRODUCTION

Paint stripping in the aerospace industry conventionally involves chemical or mechanical (abrasive) paint removal from the component's surface. Advances on alternative paint removal methods have been reviewed in Ref. [1]. Amongst the above processes, the use of laser beam scanning has drawn considerable attention, as it provides significant advantages over the conventional techniques in terms of cost savings and environmental friendliness. Paint removal rates of the order of one square meter per hour have been achieved by the use of laser scanning for both aluminum alloy and composite substrate for a paint layer of about 100 μm thickness [2]. The study of the possible effects of these novel paint removal processes on the mechanical behavior of the substrate materials has been limited. An extensive study of the effects of these novel paint removal processes on the mechanical behavior of the widely used aluminum 2024-T3 substrate material has been performed in [3]. The mechanical properties studied were tensile properties, fracture toughness and fatigue life. It was found that although there appears to be no significant effect on yield strength and ultimate tensile strength, the tensile ductility and fracture toughness degrade considerably. On the other hand, fatigue life was extended. The observed enhancement of fatigue life is attributed to the development of compressive residual stresses during the paint removal processing. To enable prediction of the fatigue behaviour of the laser beam surface treated material, the calculation of the compressive residual stresses induced by the laser beam treatment is required. Modeling of various laser beam processes have been performed in the literature, however most of the models refer to the laser beam forming e.g. [4,5] and laser beam welding e.g. [6,7]. In the present work, numerical simulation of the laser beam peening, which is applied in order to achieve paint removal is performed. A thermal transient analysis of the laser beam process is performed stepwise and the distribution of the temperature along the plate surface, as well as, through the thickness is determined. Consequently, a transient structural analysis is performed for the thermal and mechanical loading and the transient stress and strain fields are determined. The stress field at the end of the laser beam process and after cooling of the plate is achieved, represents the thermally induced residual stress field. It is then assumed that fatigue of the plate takes place under an 'effective' stress level, which is the difference between the applied stress and the residual stress. Using this assumption, the fatigue behaviour of the laser beam surface treated plate is successfully predicted.

2. EXPERIMENTAL INVESTIGATION

The material used in the present investigation is aluminum alloy 2024-T3, in sheet form of 1mm thickness. Prior to preparing fatigue test specimens, the sheets are coated using an epoxy as primer, a white polyurethane paint as top coat and acrylic finishing, similar to the paint used in the aircraft industry. Fatigue specimens have been machined according to the specifications ASTM E466-82. All specimens are cut in the long transverse (LT) direction. Specimen paint stripping has been carried out using laser radiation of excimer laser source [8] and laser radiation of CO_2 laser source [9], before the fatigue testing. The applied processes, as well as the experimental set-ups, used for stripping the specimens are described extensively in Refs. [8-9]. The set-up used for laser paint stripping involves a laser source capable of scanning the sample surface, as well as, a micropositioner guided by a suitable micropositioning controller, linked to the laser source via a computer. Following the paint removal process, the specimens are subjected to mechanical fatigue testing, corresponding to maximum stresses from 175 to 350 MPa, according to the specification ASTM E-466. Macroscopic residual stresses were measured after the laser beam surface treatment with the X-ray diffraction $\sin^2\psi$ method [10] using CrKα radiation, with an irradiated area of 0.5 mm x 4 mm with the long axis aligned parallel to the long dimension of the fatigue specimen. With regard to the fatigue behavior, the number of cycles to failure at the specified maximum stress levels for the reference material, as well as, the surface treated material are shown in Fig. 1, as reproduced from Ref. [3] in the form of the *S-N* diagram. The solid line of Fig. 1 fits the *S-N* curve of the reference material. Examination of this diagram reveals that there is an improvement in fatigue life, which depends on the paint stripping process and stress amplitude level. At high stress levels (300 MPa) the effect of paint stripping processing, beyond the expected experimental error, is low, regardless of the processing method used. At low stress levels (200 MPa), however, there is a significant improvement in fatigue life associated with the application of the paint stripping processes. There is a two- to four-fold life extension associated with excimer laser processing and more than an order of magnitude life extension associated with CO_2 laser processing.

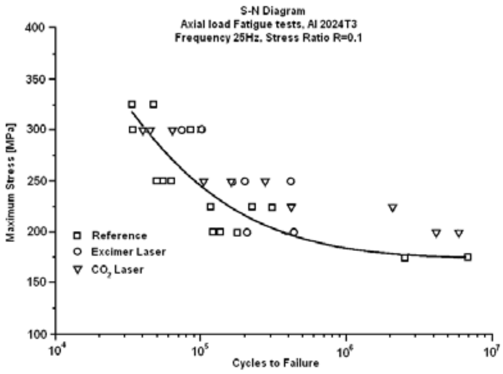

Fig. 1: *S-N* diagrams for fatigue tests of the reference and the treated Al 2024T3 specimens

To rationalize the observed behavior, residual stress calculations are performed for the three paint stripping methods. To this purpose, the paint stripping process is numerically simulated and the residual stress field, is calculated.

3. FINITE-ELEMENT SIMULATION OF THE LASER STRIPPING PROCESS

Simulation of the laser paint stripping process is complex and difficult. As analytical simulations are inadequate, a numerical model is developed to make simulation of the laser peening process manageable. The process simulation model is based on a coupled thermal-structural transient analysis. For the analysis, the finite-element code 'ANSYS' [11] is used. The simulation process occurs in four steps:
a) The first step includes the geometrical model generation phase and the input of the laser stripping process parameters b) The thermal analysis step is on of the main steps of the process simulation. The calculation of temperatures and their dependency on time, is made by using the nonlinear heat-transfer equation:

$$[C(T)]\{T^{'}(t)\} + [K(T)]\{T(t)\} + \{Q(t)\} = 0 \qquad (1)$$

where, $C(T)$ is the temperature-dependent specific-heat matrix, $K(T)$ is the temperature-dependent conductivity matrix, $Q(T)$ is the heat flux vector and $T(t)$ and $T^{'}(t)$ are the time-dependent nodal temperature and the time derivative of the nodal temperature vector, respectively. Eq. (1) is solved using the Newton-Raphson procedure and the Newmark integration method.
c) Derivation of stresses and strains occurs in a next step by solving the non-linear transient dynamic structural equation:

$$[M(T)]\{u^{''}(t)\} + [C(T)]\{u^{'}(t)\} + [K(T)]\{u(t)\} + \{F(t)\} + \{F\text{th}(t)\} = 0 \qquad (2)$$

using also the Newton-Raphson procedure and the Newmark integration method. In Eq. (2), $M(T)$, $C(T)$ and $K(T)$ are the temperature-dependent mass damping and stiffness matrices; $F(t)$ is the

external load vector; $F_{th}(t)$ is the temperature load vector; and $\{u(t)\}$, $\{u'(t)\}$ and $\{u''(t)\}$ are the displacement, velocity and acceleration vectors, respectively. Plasticity is accounted for by means of an iterative process to obtain the elements where the Von-Misses stress σ_{eq} has reached the yield point σ_y. d) Finally, the simulation process also includes a coupling interphase of the thermal and the structural analysis steps. The basic assumptions of the present simulation model can be summarized as: (i) A heat flux quantity $q = A\ Q$ acts on an area $F = d^2$ for the time $t = d/v$, where Q denotes the laser beam energy, d the beam diameter, v the laser travel speed and A the absorption coefficient.
(ii) The laser beam energy Q follows a Gaussian distribution. (iii) Cooling of the irradiated material occurs through free convection to air. (iv) Variation of thermal conductivity, specific heat and density with temperature has been considered by means of linear interpolation using the data provided in [12,13]. (v) For the plastic yielding, the von Mises criterion has been used. (vi) The hardening effect on the material behaviour is included, the material stress-strain behaviour being approximated by means of a bi-linear curve with sloped depending on temperature. (vii) The temperature dependency of Young's modulus and Poisson's ratio has been taken into account by means of linear interpolation using data from [12,13]. (viii) The dissipation of energy due to plastic deformation can be neglected when compared with the energy involved during the thermal process. The overall computing time depends strongly on the selection of the integration time interval Δt, which influences also the accuracy of the analysis. To reduce computing time, optimization has been made to increase Δt such that no remarkable drawback in accuracy occurs. For the application of the proposed algorithm, the basic parameters required are the plate dimensions, laser power, laser travel speed, laser beam diameter, material absorption coefficient and the material properties. The computed results include: (i) the time-dependent temperature distribution; (ii) the time-dependent stresses, strains and distortions; (iii) the residual stresses and strains; and (iv) the final shape. In all cases the calculated residual stresses are compressive. The computed values are compared to the experimentally measured values of the residual stresses that appear in Table 1. The highest compressive residual stress is associated with CO_2 laser radiation, followed by excimer laser radiation. The computed results have been found in a good agreement with the experimental ones.

Table 1: Compressive residual stresses for various paint removal methods examined

Paint removal method		Compressive residual stress (MPa)			Average
		At max fatigue stress of:			
		200 MPa	250 MPa	300 MPa	
Experimental	CO2 laser	45±2	44±4	46±4	45
	Excimer laser	19±5	20±5	20 ±5	20
Numerical Simulation	CO2 laser				42
	Excimer laser				18

4. DISCUSSION OF THE FATIGUE BEHAVIOUR PREDICTION OF THE LASER BEAM TREATED MATERIAL

The residual stress results presented in section 3 provide useful means to rationalize the observed fatigue behavior. The structural changes caused by the stripping processes, i.e., increase of the residual compressive stresses tend to extend fatigue life. Generally, in high cycle fatigue (HCF), total fatigue life is controlled by fatigue crack initiation rather than by crack propagation. The crack initiation phase, as a percentage of the total fatigue life, depends on the stress amplitude and increases with decreasing stress level; the contribution of the fatigue crack growth phase to the total fatigue life becomes appreciable when stress amplitude levels become medium or high. The predominant factor for the observed extension of the fatigue life after the laser treatment is the development of compressive residual stresses. The larger the magnitude of these stresses, the larger is the effect in extending fatigue life. Referring to Fig. 1 and Table 1, the observed fatigue life enhancement is fully compatible with the magnitude of the residual stresses: it is highest in CO_2 laser treatment, followed by excimer laser treatment. At low stress levels, the depth of material modified by the laser or paint stripping processes is greater than the fatigue crack initiation process zone, thus affecting fatigue life beneficially. The experimental results suggest that, at low stress amplitudes, a longer fatigue life extension is associated with CO_2 laser processing. It is believed that this difference in behavior is associated with the fact that the CO_2 laser emits in the infrared, whereas the excimer laser emits in the ultraviolet. This suggests that the CO_2 laser has a more pronounced thermal effect than the excimer laser; it results in a deeper thermally affected and modified zone, thus affecting fatigue behavior significantly with the development of compressive residual stresses also calculated by the thermal model. The excimer laser has better absorptivity and coupling with the metal surface, but the effects are limited to a very thin surface layer. At high stress amplitudes, the fatigue life is controlled by fatigue crack growth rather than by fatigue crack initiation, thus the impact of near-surface residual stresses on fatigue life becomes smaller. The number of cycles for fatigue failure for all stripped specimens examined in this work are summarized again in Fig. 2; they are displayed at the specified maximum stresses reduced by the residual compressive stresses calculated for the respective laser beam treatment method. For comparison, the fatigue life obtained for the reference specimens at the specified maximum stresses has also been included. The results imply the simplification that the compressive residual stresses are acting through the total fatigue life; however, one should recall the predominant role of the fatigue crack initiation phase in the total fatigue life at HCF conditions. The results of Fig. 2 demonstrate the significance of the compressive residual stresses developed for the fatigue behavior of the stripped specimens; the *S-N* curves of the stripped specimens fit to the *S-N* curve of the reference material well within the experimental scatter range.

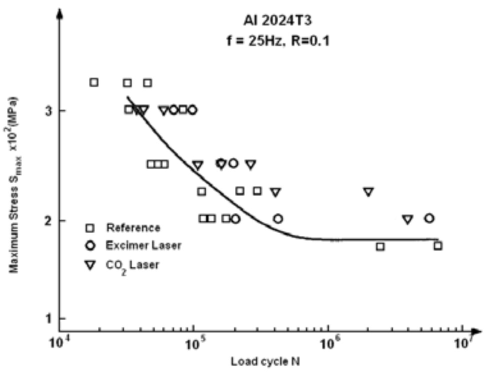

Fig. 2: *S-N* diagrams for fatigue tests of the reference and the treated Al 2024T3 specimens. (The data points for the treated specimens have been displaced downwards, relative to Fig. 1, by an amount

corresponding to the compressive residual stress measured for each paint removal method)

5. CONCLUSIONS

Numerical simulation of the laser stripping process has been performed by a coupled thermal-structural transient analysis using the finite-element method. The main purpose of the simulation is the prediction of the residual stress field of the laser beam surface peening process. Experimental and computed results correlated well. By making use of the computed residual stress field, the effect of two laser stripping processes on the fatigue behavior of aluminum alloy 2024 is assessed. The paint removal processes investigated include excimer laser and CO_2 laser surface treatment. It is concluded that the observed enhancement of fatigue life can attributed to the development of compressive residual stresses during the laser stripping processing. At low stresses, the magnitude of the residual stress correlates with the relative enhancement in fatigue life for the three processes investigated.

REFERENCES

[1] Environmentally safe and effective processes for paint removal, Agard report LS-201, 1995.
[2] BRITE/EURAM No 0151, New techniques on paint removal, Final report, CEC, Brussels, 1996.
[3] Pantelakis Sp.G., Haidemenopoulos G.N., "Effect of novel paint removal processes on the fatigue behavior of aluminum alloy 2024", Surface and Coatings Technology 106, pp. 139-146, 1996.
[4] Frackiewicz H., Trampczynski W., Przetakiewicz W., "Shaping of tubes by laser beam:" ISATA 25th, pp. 373-380, 1992.
[5] Kyrsanidi An. K., Kermanidis Th. B., Pantelakis Sp. G., "Numerical and experimental investigation of the laser forming process", J. of Material Processing Technology ,87, pp. 281-290, 1999.
[6] Tsirkas S.A, Papanikos P., Kermanidis Th., "Numerical Simulation of the Laser Welding Process in Butt-joint specimens", Journal of Materials Processing Technology, 134(1), pp. 59-69, 2003.
[7] Tsirkas S.A., Papanikos P., Pericleous K., Strusevich N., Boitout F.,. Bergheau J. M, "Evaluation of distortions of laser welded shipbuilding parts using a local-global finite element approach, Science and Technology of Welding and Joining", 8(1), pp. 79-88, 2003.
[8] Dornier Luftfahrt GmbH contribution, in: BRITE/EURAM No.0151, New techniques on paint removal, Final report, CEC, Brussels, 1996.
[9] Centro Laser SCRL contribution, in: BRITE/EURAM No.0151, New techniques on paint removal, Final report, CEC, Brussels, 1996.
[10] Hilley M.E. (Ed.), Residual Stress Measurement by X-Ray Diffraction, SAE 784a, Society of Automotive Engineers, Warren-dale, PA, p. 20, 1971.
[11] ANSYS: User's manual, ver. 7.1, Swanson Analysis Systems Inc., 2004.
[12] Papazoglou V., Analytical techniques for determining temperatures thermal strains and residual stresses during welding, PhD thesis, Massachusetts Institute of Technology, 1981.
[13] Aerospace Structural Metals Handbook Vol. 1. Ferrous Alloys, Technical Report, ASD-TDR-63-741(Vol.I)(Suppl.I), Weiss V.,Sessler, J.G. eds. 1963.